Plasma Sources Science and Technology

PAPER

Positive double-pulse streamers: how pulse-to-pulse delay influences initiation and propagation of subsequent discharges

To cite this article: Y Li *et al* 2018 *Plasma Sources Sci. Technol.* **27** 125003

View the article online for updates and enhancements.

IOP ebooks™

Bringing you innovative digital publishing with leading voices to create your essential collection of books in STEM research.

Start exploring the collection - download the first chapter of every title for free.

This content was downloaded from IP address 131.155.2.68 on 08/01/2019 at 11:16

IOP Publishing Plasma Sources Science and Technology
Plasma Sources Sci. Technol. 27 (2018) 125003 (15pp) https://doi.org/10.1088/1361-6595/aaf2c6

Positive double-pulse streamers: how pulse-to-pulse delay influences initiation and propagation of subsequent discharges

Y Li[1,2], E M van Veldhuizen[2], G J Zhang[1,4], U Ebert[2,3] and S Nijdam[2,4]

[1] State Key Laboratory of Electrical Insulation and Power Equipment, Xi'an Jiaotong University, Xi'an 710049, People's Republic of China
[2] Department of Applied Physics, Eindhoven University of Technology, PO Box 513, 5600 MB Eindhoven, The Netherlands
[3] Centrum Wiskunde & Informatica (CWI), Amsterdam, The Netherlands

E-mail: gjzhang@xjtu.edu.cn and s.nijdam@tue.nl

Received 24 August 2018, revised 22 October 2018
Accepted for publication 21 November 2018
Published 24 December 2018

Abstract

Residual charges and species created by previous streamers have a great impact on the characteristics of the next discharge. This is especially pronounced in repetitively pulsed discharges, where the physical and chemical reactions during the decay phase play a very important role. We have performed double-pulse streamer experiments in artificial air and pure nitrogen with a varying pulse delay (Δt) from 0.45 μs to 20 ms. We have observed morphological transformations of the 2nd-pulse streamer as a function of Δt and classified six typical stages by streamer length. The propagation distance of the 2nd-pulse streamer can be 66% longer than the 1st-pulse in 66.7 mbar nitrogen, while it is 37% longer in air under the same conditions. However, we find that the longer propagation distance of the 2nd-pulse streamer in N_2 is not caused by a higher velocity nor by fast gas heating of previous channels under our experimental conditions, but by earlier inception which gives more time to propagate during the pulse. In air, on the other hand, the streamers initiate almost at the same time in both pulses but the inception cloud of the 2nd-pulse streamer breaks up earlier. The onset of every stage occurs at smaller Δt in air than in N_2 at the same pressure. These observations imply that different mechanisms work in N_2 and air, e.g. photoionization and attachment.

Keywords: streamer discharge, double-pulse, background ionization, inception time

1. Introduction

It is generally acknowledged that positive streamers require a source of electrons in front of them in order to sustain their propagation. The electron sources can vary such as photoionization [1, 2] or residual electrons and ions from previous discharges [3] or from laser illumination or radioactive additives [4]. These electron sources except for photoionization can be classified as background ionization that already existed before the streamer occurrence. The easiest way to create a background ionization level above the natural level is by previous discharges. After the discharges, the seed electrons can be provided directly or by de-excitation of molecules or atoms in excited states, by collision between metastable species , detachment from ions [5], etc. This is the reason why the threshold electric field for discharge inception in a gas during repetitive bursts is lower than for a single pulse, which has been frequently observed, and nanosecond repetitively pulsed discharges have been intensively used in applications [3, 6–9].

It is expected that species created by the repetitive pulses will remain in the electrode gap, including positive ions, negative ions, and neutral species like vibrationally excited molecules and electronically excited metastable states [6, 10, 11]. Acker and Penney [12] observed that successive streamers of repetitive discharges at room temperature and

[4] Authors to whom any correspondence should be addressed.

 © 2018 IOP Publishing Ltd

pressure follow the same path, and that their propagation speed is greater than of streamers following differing paths. The observations also suggest that whether streamers follow the same path depends on the time interval between consecutive streamers. Acker and Penney proposed that uncharged metastable products left behind by previous streamer discharges can be ionized by collision more easily than oxygen or nitrogen in the ground state. The subsequent streamer, if triggered before the metastable products are dispersed, can follow the trail of the earlier streamer and might propagate faster because of a greater net positive charge in the streamer tip. Hartmann and Gallimberti [13] interpreted that the high metastable concentration enables the electrons in the avalanches developing in the active region, to undergo a large number of superelastic collisions between electrons and metastable molecules and to gain energy by deactivation of the metastable states. Hence, this enhances the avalanche development and affects the streamer propagation characteristics.

Dozens of metastable species that exist in pure N_2 and N_2–O_2 mixture discharges, such as metastable atoms $N(^2D)$, $N(^2P)$ and metastable $N_2(A^3\Sigma_u^+)$ molecules, are believed to influence the discharge by providing electrons [10, 14, 15]. These metastables are with the lowest molecular metastable level and long lifetime (∼several seconds) under very low pressure (1.33 mbar) [16]. The radiative lifetime of these states can be long and depend on pressure [10].

Geary and Penney [17] show the occurrence of a heated channel in positive point-plane gaps by interferometry. Heated air has a lower density and therefore guides subsequent streamers and causes them to propagate more energetically. Popov [18] presents a model of fast heating of nitrogen–oxygen mixtures excited by a gas discharge in a broad range of reduced electric fields ($\boldsymbol{E}/n \leqslant 1000$ Td). The model approximates the fraction η_E of discharge energy spent on the excitation of electronic degrees of freedom, ionization and dissociation of molecules that can be converted to fast heating ($\eta_E \sim 30\%$ for discharges in air).

How previous discharges exactly influence subsequent ones is of great interest in plasma physics and chemistry and the subject of this paper. In previous work, we have presented double-pulse experiments in nitrogen (N_2), artificial air and argon at 67 mbar to 533 mbar with varying pulse delay, Δt, between the first and the second pulse, i.e. from 200 ns to 40 ms [19]. The advantage of using double-pulse voltage shapes instead of multi-pulses is that it allows us to investigate a huge range of pulse-to-pulse intervals without the need of too complex or high-power pulsers. When adjusting the pulse delay between two voltage pulses, it can be regarded as generating a repetitively pulsed voltage for which frequency is dependent on pulse delay and pulse width.

In the previous work [19], we found that the 2nd pulse streamer would continue the paths of the first-pulse streamers, and we called streamer continuation, when the delay between the two pulses, Δt is below 0.5–15 μs at 133 mbar in different N_2–O_2 mixtures, and, according to our plasma-chemical modeling, this time is determined by the electron loss rate which has a minimum around 0.2% oxygen concentration in N_2–O_2 mixtures. For increasing values of Δt, we observed that for Δt just above these values no new streamers occur at all, while for even larger Δt streamers created by the 2nd pulse start to show up and will follow the paths of old channels. For larger Δt (10–200 μs) the new streamers start to increase in size and move to the center of the old channels. Finally, around millisecond timescales the new channels are completely independent of the old channels.

This paper follows up on this work and further investigates how the previous discharge exactly influences the subsequent one in nitrogen and artificial air at 66.7–400 mbar pressure (1 mbar = 100 Pa). We aim to clearly classify the varying stages of the second pulse discharge with increasing pulse delay (Δt) in air and nitrogen and we measure the streamer propagation length, velocity and inception time, in order to provide quantitative evidences that can be used to interpret various phenomena in each stage.

An important difference in experiment between our previous work and the work described here is that we now could not make use of two (identical) ICCD cameras to image the two subsequent discharges individually. However, we could make use of a stroboscopic ICCD camera which provided other exciting possibilities.

This paper is organized as follows: the experimental set-up, applied conditions and diagnostic methods are treated in section 2. Section 3 gives a general description of streamers continuation in double pulse experiments. In section 4, a detailed evolutional progression of continuing streamers with varying Δt is shown and analyzed in air and nitrogen for varying pressures. We extract velocity, inception time and discharge current during the double-pulse streamers and compare with the varying stages in section 5. The summary and conclusions are achieved in section 6.

2. Experimental set-up and methodology

All measurements described here have been performed in a point-plate electrode geometry with 160 mm gap distance inside a vacuum vessel. A detailed description of the vessel can be found in our previous publication [4]. The background pressure in the vessel can reach as low as 3×10^{-7} mbar. In our experiments, nitrogen (N_2) and artificial air (80% N_2 + 20% O_2) are used, both of 6.0 purity, i.e. with less than 1 ppm impurity. Before the measurement, the leak-rate (including outgassing) of the vessel is tested and found to be 2×10^{-5} mbar min^{-1}. This suggests that the impurity level inside the vessel is less than 50 ppm in total during most measurements (assuming a working pressure of 100 mbar and an experimental duration of less than 200 min). This is a higher impurity level than in earlier experiments in this vessel due to a recent move of the set-up and the installment of new tubing, which was not fully leak-tested at the time of the experiments. The measurements are performed in static gas for a few hours (no gas flow is used).

To study how previous discharges influence subsequent ones, we used a double-pulse voltage wave-shape produced by a push-pull switch, Behlke HTS 651-10-GSM. One of the

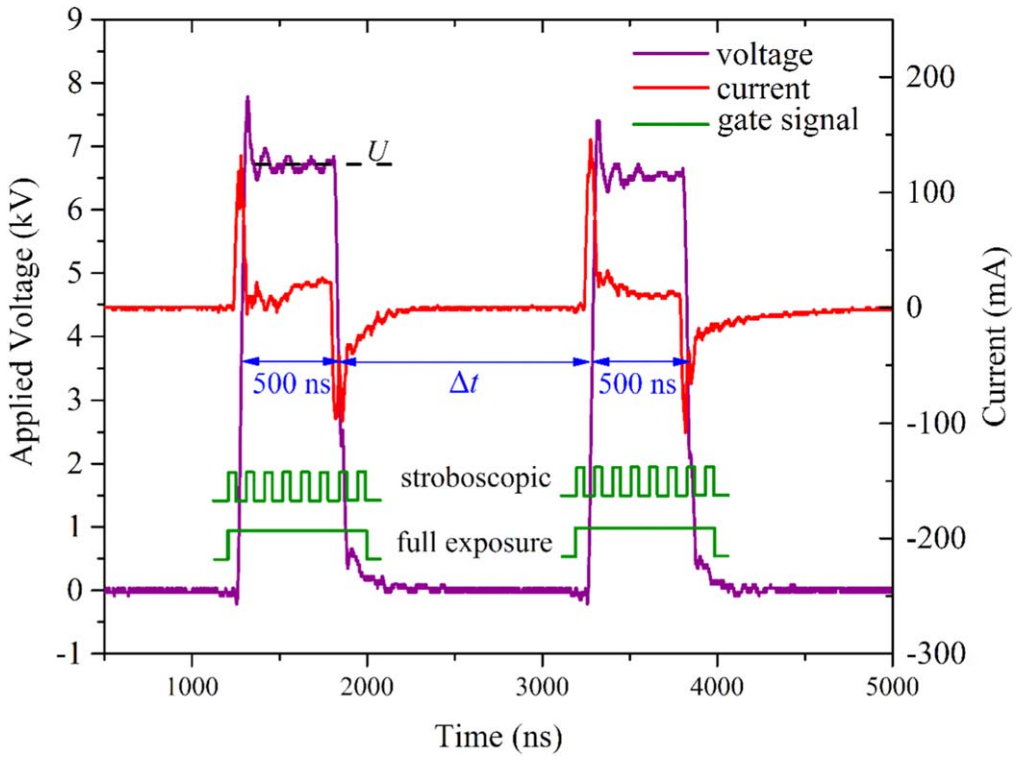

Figure 1. Typical double-pulse voltage, current and two kinds of imaging techniques (full exposure and stroboscopic imaging). The shown example has 6.6 kV voltage, pulse lengths of 500 ns and a pulse-to-pulse delay $\Delta t = 1.4$ μs in 100 mbar pure nitrogen.

advantages of such a solid-state switch is that it can generate pulsed voltage with very low jitter, which enables us to have two nearly identical pulses. Figure 1 plots an example of the double-pulse voltage shape we used in the experiment. The rise time of the pulsed voltage is around 30 ns and the pulse width is 500 ns. The minimum pulse width that the solid switch can generate is 300 ns, but in our experiments, we have fixed the width to 500 ns and have chosen the voltage amplitude for each gas pressure such that the streamers pass roughly half the gap during the 1st pulse. The difference in voltage amplitude between two paired pulses is less than 5% which is due to the recharging of the capacitors. The delay between the two pulses, Δt, can be set with a function generator. The current is acquired via a non-inductive resistor of 50 ohm connected to the cathode electrode and an attenuator with a factor of 30 db.

A PicoStar HR12 ICCD camera system is used for optical diagnostics of the streamer discharge. This system is capable of both long exposures as well as stroboscopic imaging with gate widths of less than 0.3 ns. We supply either a full pulse width or a short train of trigger pulses to the intensifier of the camera as shown in green in figure 1. As a streamer primarily emits light from the head region where it grows, the image then shows either the complete channel that has grown during the exposure time or a sequence of subsequent head images at the respective head positions in a stroboscopic manner [20].

The streamer propagation length and velocity are measured by either full exposure or stroboscopic imaging techniques as described in figure 2. We use stroboscopic images (see figure 2(c)) to calculate velocities of streamers by determining the distances that streamer heads move between subsequent camera gate periods. This method enables us to calculate the propagation velocity of every streamer branch with high accuracy, leading to a distribution of propagation velocities in one discharge event instead of merely an average one. However, it should be pointed out that the velocities in this paper are obtained from two stroboscopic exposures, while in figure 2 we show four exposures for demonstration purposes. The average velocities of streamers are calculated via the ratio of longest traveled distance within the gate interval.

Even though 2D images have high resolution, it is inevitable that the projection of a streamer to a 2D image is often shorter than its real length. These problems would lead to an underestimation of the velocity. In previous work we have implemented stereo-photographic techniques to reconstruct a 3D image showing a promising tool to investigate velocities, branching angles and reconnections of multichannel discharges [21]. However, in this paper, we still use 2D pictures to obtain the parameters but the following measures are taken to counteract the error:

(1) Choose conditions where streamer lengths can be measured reliably, if possible about half of the electrode gap distance since streamers that are too short or too long would increase the unreliability of the measurement. We attempt to keep U/p (with U the applied voltage and p the operating pressure) constant between experiments in order to get similar discharge dimensions. Actual used values are listed in table 1. This

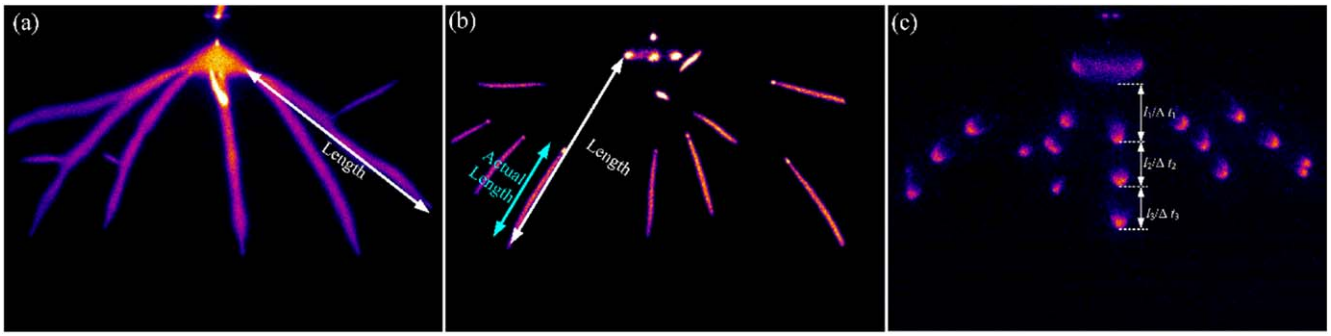

Figure 2. The streamer propagation length (a) from the inception cloud, and (b) actual length from the stopping point of the 1st pulse streamer. Both (a) and (b) are measured by full exposure. Velocities are obtained by stroboscopic images (c) of streamer discharges. This example shows streamers in 100 mbar artificial air at 8.5 kV. For the length measurements, the straight distance of the longest branch is selected (see (a) and (b)); while the velocity is calculated by the ratio between distance of two streamer heads from a channel and the exposure interval (see (c)). Here, the exposure time is set to 10 ns and the delay between exposures to 100 ns so $\Delta t_1 = \Delta t_2 = \Delta t_3 = 110$ ns. This technique enables us to calculate the streamer propagation velocity with high spatial resolution.

Table 1. Experimental conditions used for a close U/p.

p (mbar)	U (kV)	U/p (kV mbar^{-1})
66.7	6.6	0.1
100	8.5	0.085
200	17	0.085
400	28	0.07

scaling is based on the similarity laws in which a constant reduced electric field $\boldsymbol{E}/n$ would lead to a similar discharge [22].

(2) Among the multiple branches in a streamer image, straight and long channels are much easier to process and interpret. Also, streamer branching may cause some channels to propagate faster than others. In fact, according to our statistics from thousands of datasets, some branches could propagate up to three times faster than the slowest branches in the same discharge event. Thus, the longest branch is chosen and the fastest velocity of branches in each discharge images is used.

(3) All the data points shown in this paper are averages with standard deviation from at least 30 separate discharge images. Those images that we pick out for data processing presented in this paper are from over 70 discharge events for each condition. Because of the inevitable stochasticity of streamer discharges, we eliminate those discharge images with obviously short propagation lengths, possibly caused by late initiation.

We define the streamer propagation length as the straight distance between the start point since breaking free of the inception cloud[5] and the end point. When the 2nd pulse streamer reignites from the stopping point of the 1st pulse discharge instead of initiating from the needle tip (in N_2) or inception cloud (in air), one should be aware that the actual propagation length is much shorter as is shown in figure 2(b). However, we still choose the 'start point' described in figure 2(a) and measure the normalized length for consistent consideration, but this will have no influence on the velocity calculation. Finally, note that all images presented in this paper have been adjusted for optimal visual quality and their color scale has no direct physical meaning.

[5] An ionization cloud initiated from electrode tip has been frequently observed in positive discharges at low pressure air. It will develop into a growing shell and eventually break up into streamers and then propagate forwards [23].

3. General phenomenon description

We have seen in [19] that discharge channels would reignite and extend their paths as long as the interval between two voltage pulses is so short that the electron density is still high enough. Figure 3 presents typical examples of streamer discharges excited by a double-pulse-voltage with $\Delta t = 0.45$ μs. Streamer continuation is also visible in full exposure images acquired during both pulses as is shown in panels 3(c) and (f). This issue essentially concerns how the leftover electron density influences the succeeding discharge, which has been of great interest for the physical community. It is clear that the reignited channels are thinner than the old paths. The discharge in air has a pronounced inception cloud around the needle tip due to photoionization [24] while this is not visible in nitrogen. Why the 2nd pulse streamer continues the previous streamers' paths and how the 1st pulse streamer discharge plays a role in subsequent streamer formation and propagation will be presented in detail in section 4.

It is worthy to point out that the reignited (or continuation) streamer produced by the second voltage pulse is not a secondary streamer, which usually denotes re-ignition of part of an existing streamer channel after it has bridged the gap. Secondary streamers can be frequently observed under DC voltage or long width pulse conditions (over several μs) [25, 26], after which a spark would usually be expected to follow.

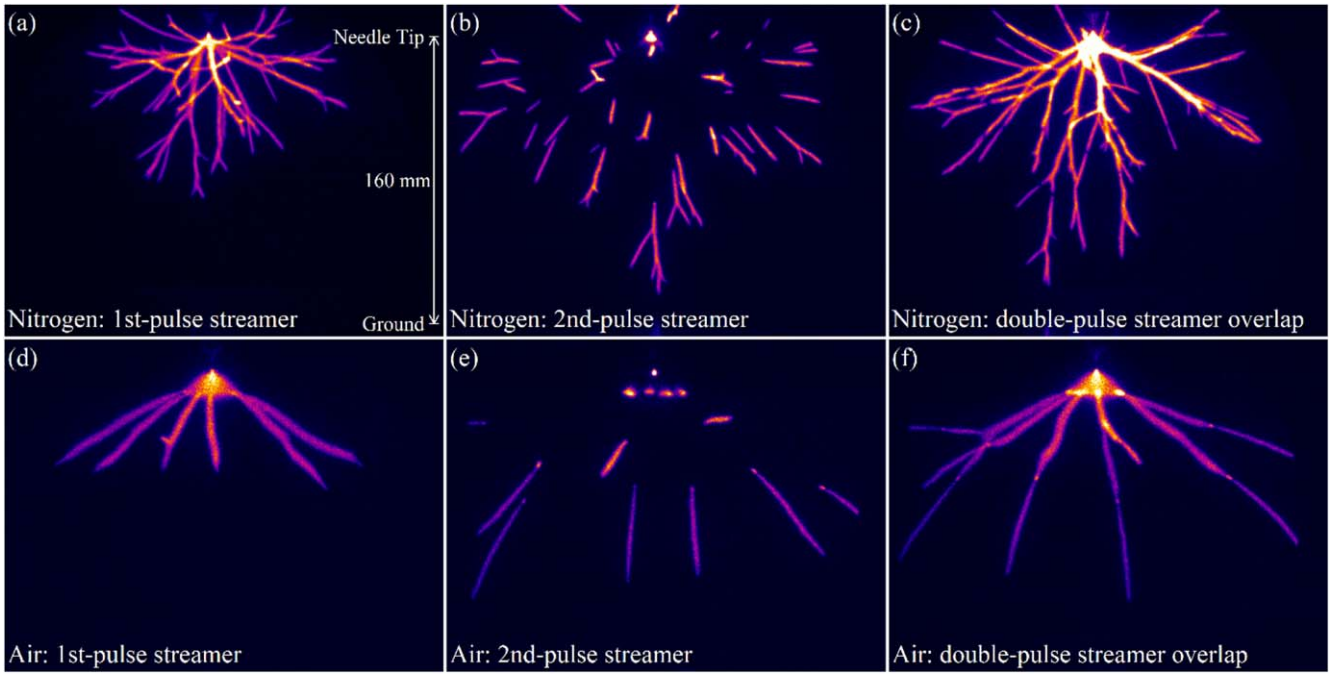

Figure 3. Streamer generation and reignition by double-pulse excitation with two voltage pulses of 8.5 kV amplitude, 500 ns pulse width and 0.45 μs delay between the pulses. The upper row is for nitrogen, and the lower row for artificial air, both at 100 mbar. Panels (a) and (d) show the streamer evolution during the first pulse, panels (b) and (e) during the second pulse, and panels (c) and (f) are full exposure images of the first and second voltage pulse together. Note that each image presents an independent discharge event.

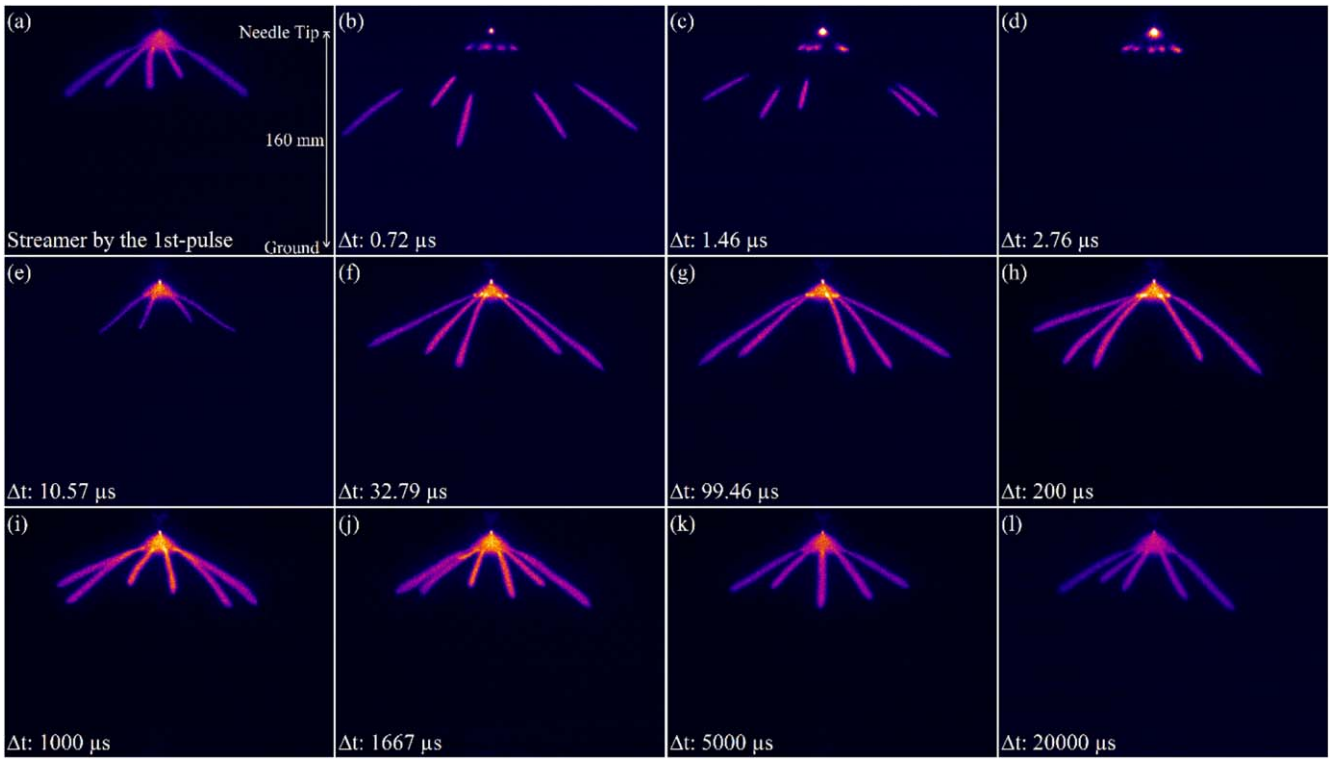

Figure 4. First pulse streamer (panel (a)) and second pulse streamers (panels (b)–(l)) in 66.7 mbar artificial air with varying pulse-to-pulse delay (Δt) with 6.6 kV amplitude and 500 ns pulse width.

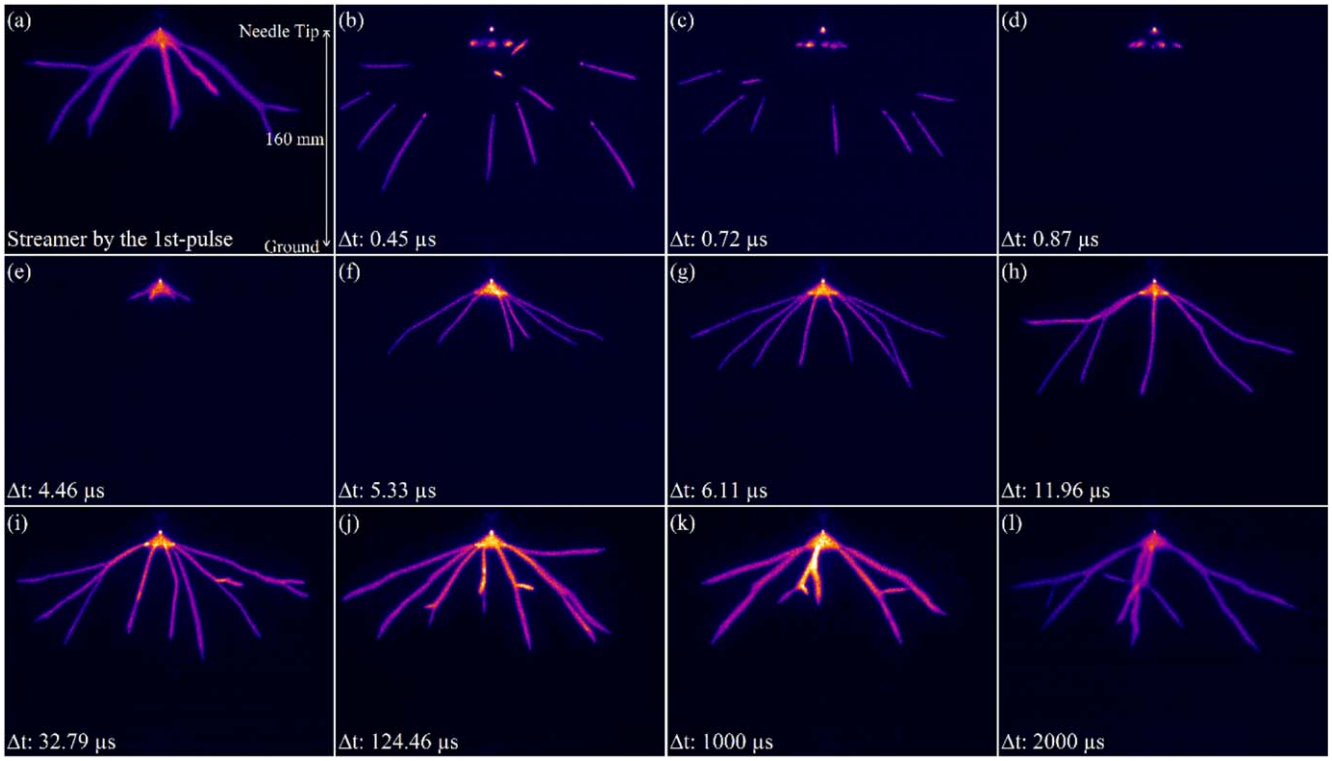

Figure 5. The same as figure 4, now in 100 mbar artificial air with 8.5 kV voltage amplitude.

4. Properties of 2nd pulse streamers as a function of Δt

Here we discuss how the streamers initiate and propagate during the second voltage pulse and how this depends on the pulse delay Δt, both in artificial air and in high purity nitrogen.

4.1. Artificial air

Figures 4 and 5 show streamers in 66.7 and 100 mbar air, respectively, for a pulse delay varying from 0.45 μs to 20 ms. The respective voltage amplitudes are consistent with table 1. Panel (a) in both figures is a typical discharge produced by the first voltage pulse; the other panels show the streamers during the second pulse, with growing delay to the first one as indicated. Since the double-pulse voltage is applied with a frequency of 1 Hz, we assume that the density of the charged particles and metastable molecules becomes so low after 1 s that it would hardly enhance the background ionization level for the first pulse discharge. In fact, our previous numerical results [4] have shown that the ionization density in 200 mbar pure nitrogen drops from over 10^{13} cm^{-3} at end of the discharge to $\sim 10^5$ cm^{-3} after 1 s.

We have measured the streamer propagation length as defined in figure 2(a) and plotted it as function of Δt in figure 6. The results correspond with the trends visible in figures 4 and 5. We here classify the stages by streamer length as function of Δt instead of the more phenomological definitions used in [19], although the resulting stages are nearly identical. We can distinguish the following six stages:

(I) The 2nd pulse streamers continue the paths left by the 1st pulse streamers and start from the stopping points of the first-pulse streamers (see figures 4(b), (c) and 5(b), (c)). This implies that the space charge of the streamer is neutralized after the end of the first voltage pulse and formed again when the second voltage pulse is applied. This streamer continuation is possible only if the first streamer channel is still sufficiently conducting after the pulse delay time Δt, as discussed in [19], and this is the case for $\Delta t < 2.7$ μs at 66.7 mbar and for $\Delta t < 0.8$ μs at 100 mbar. Higher pressures (densities) do not only shorten the mean free path of particles, but also decrease the electron attachment time, and hence the decay time of the plasma conductivity.

(II) For a delay time Δt just a bit longer than for streamer continuation (stage I), no real streamer discharges are observed, and only some luminous dots emerge from the needle tip and from the edge of the inception cloud (see figures 4(d), 5(d)). These bright dots are already visible in stage (I). They are located around the electrode tip and on the outer envelope of the inception cloud where a strong electric field can initiate new avalanches locally. This region is bright in all images, which indicates a high impact ionization rate which results from the coincidence of a high field and a high electron density. The high conductivity of this area shields the potential of the electrode and thereby suppresses the occurrence of new streamers.

(III) In this stage, new streamers start to grow from the tip-region. However, we observe that during a very short time regime (Δt typically less than 3 μs in 100 mbar

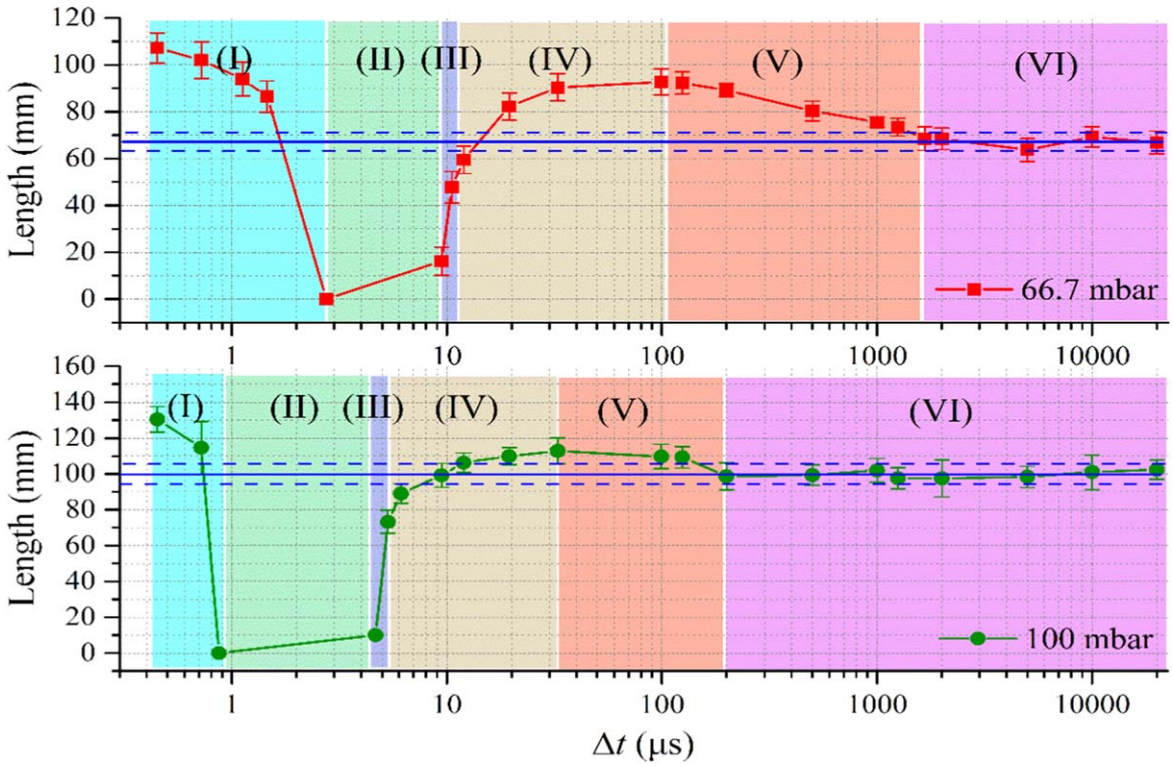

Figure 6. The 2nd pulse streamer length as a function of the pulse delay time Δt in artificial air at 66.7 and 100 mbar, corresponding to figures 4 and 5. The solid and dashed blue lines represent average and standard deviation of the length of the 1st pulse streamers. Note that in stage (I), the propagation length of streamers is measured from the edge of inception cloud and that a length of 0 indicates that no new streamers are visible.

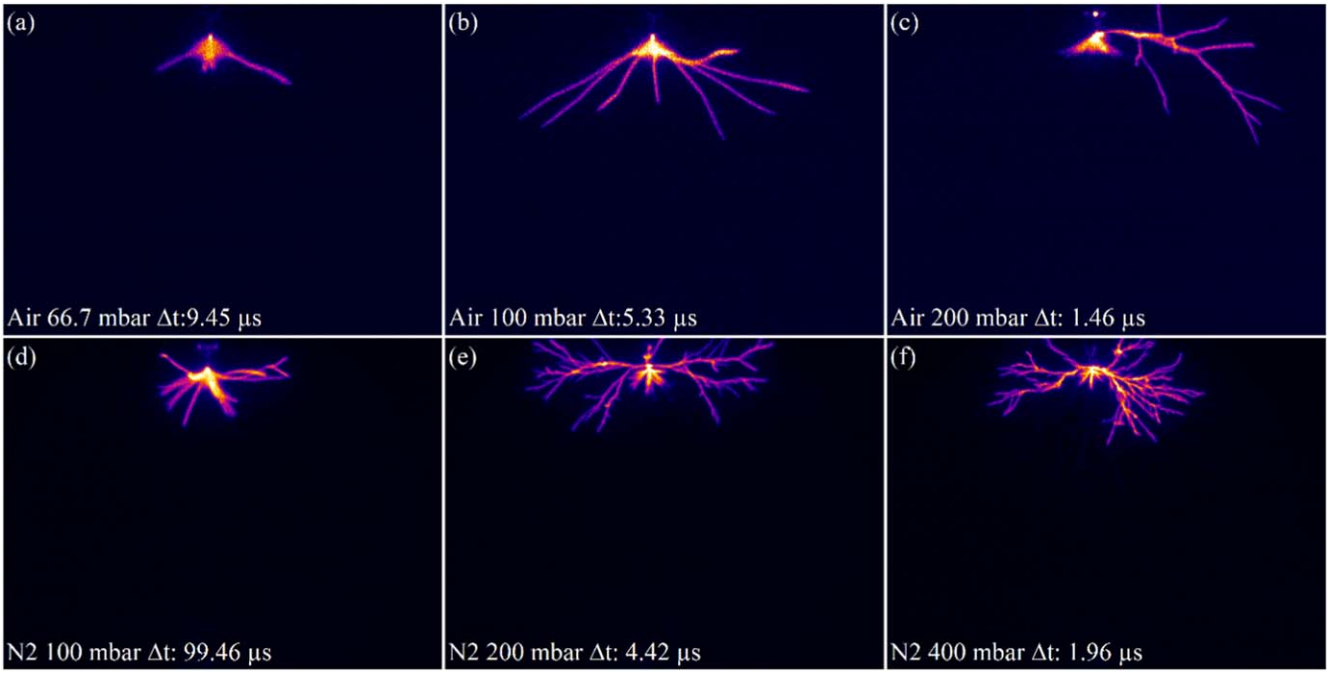

Figure 7. Side-propagating streamers observed at varying pressures from 66.7 mbar to 400 mbar in air and nitrogen.

air) new streamers have a strong tendency to propagate sideward instead of following the lines of the background electric field. We show some of these side-propagating streamers at varying pressures in figure 7. They are especially remarkable for pressures over 200 mbar. This phenomenon has seldom been reported in literature. Phenomenologically, these side-propagation streamers are alike the so-called late streamers of Briels *et al* [27] in 2006 that emerged from the tip holder above other, earlier streamers during the same voltage

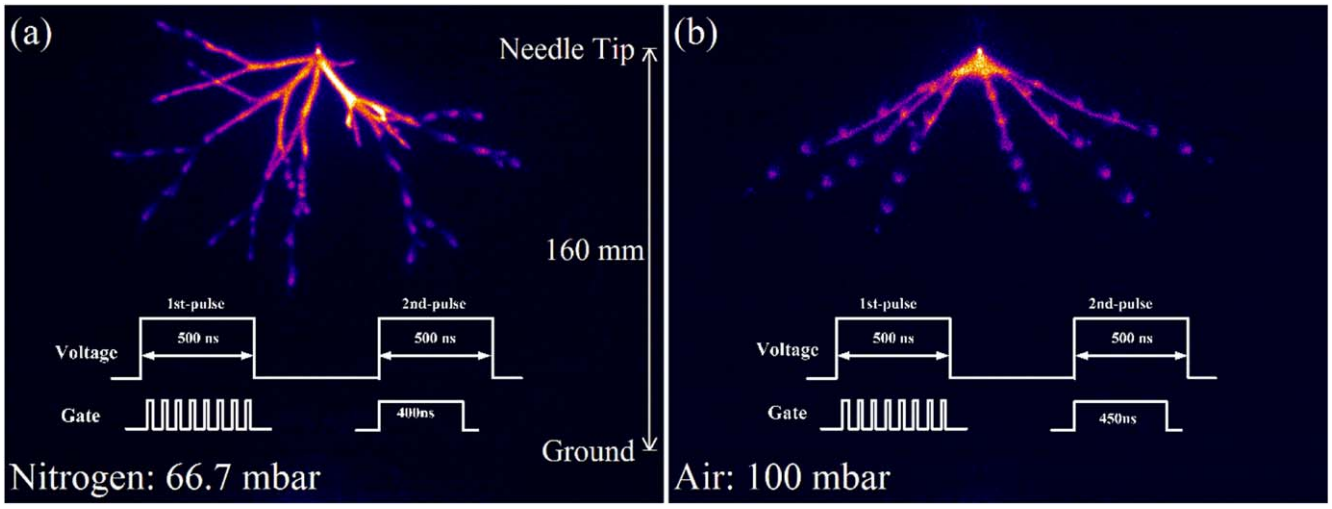

Figure 8. Joint usage of stroboscopic exposure and full exposure during the double-pulse in one image. (a) Nitrogen of 66.7 mbar, $U = 6.6$ kV and $\Delta t = 200$ μs; 8 exposures of 10 ns width and 60 ns camera gate closing time between each exposure during the 1st pulse; 400 ns exposure time during the 2nd pulse. (b) Air of 100 mbar, $U = 8.5$ kV and $\Delta t = 4.46$ μs; 8 exposures of 10 ns width and 60 ns camera gate closing time between each exposure during the 1st pulse; 450 ns exposure time during the 2nd pulse.

pulse and then bend towards an existing streamer path. However, we check whether our sideward streamers initiate from the electrode tip or from its holder. According to figure 7, it is clear that our side-propagation streamers start at the tip and propagate sideward; which makes them different than the late streamers. The side-propagation is followed by a new stage of extinction and soon turns to the forward propagation streamers.

(IV) For longer Δt (e.g. >11.45 μs in 66.7 mbar air), the shielding by the remaining electrons becomes so weak that new streamers can grow again in the area occupied by the 1st pulse streamers (see figures 4(e) and 5(e)).

Interestingly, the 2nd pulse streamers mostly follow the trails of the 1st pulse streamers. We verified this by jointly using stroboscopic exposure and full exposure techniques during the double-pulse to have one image as depicted in figure 8. The method enables us to have two streamer discharge events in one ICCD image and to check the correlation between them. The specific approach is as follows. We use stroboscopic exposure (8 exposures with 10 ns each) during the 1st pulse and long exposure during the 2nd pulse as indicated in figure 1. This is an optimized imaging solution because the 1st pulse streamers are generally thicker, but the dotted images of the 1st pulse streamers will not fully cover the branches of the 2nd pulse streamer even if they follow the same trails. The long exposure during the 2nd pulse is less than the full width of the voltage pulse so that the 2nd pulse streamers are not too long and do not fully cover the trace of their predecessors, see figure 8(a).

The resulting images in nitrogen and air indicate that the 2nd pulse streamers follow the 1st pulse streamers due to the enhanced electron density or enhanced ionizability within the old paths. It is especially clear that they propagate along the edge of the 1st pulse streamers in air. We believe that the streamers cannot enter the area of high leftover electron density of the old channel because they cannot enhance the field there but preferentially follow the intermediate electron density levels present at the edge of these channels [19]. Phenomenologically, they are reminiscent of the experiments described in [28] where we used a very low level of laser induced pre-ionization ($\leqslant 10^9$ cm^{-3}) to generate streamers that can be guided in a direction nearly perpendicular to the background field.

Another remarkable feature in this stage is that the maximum length of the 2nd pulse streamers increases with Δt, and can exceed their pioneers (see figures 4(a) versus (f)–(h) and 5(a) versus (h)–(j)). In 66.7 mbar air, the length increasing stage starts at $\Delta t = 11.96$ μs and the 2nd pulse streamers reach their maximum length of 92.7 ± 5.5 mm at $\Delta t = 100$ μs, which is 37% longer than the 1st pulse discharge streamers. In 100 mbar air, this stage starts at $\Delta t = 6.1$ μs and at $\Delta t = 32$ μs streamers reach the maximum distance of 122.7 ± 7.2 mm, which is 15% longer than the 1st pulse discharges.

When Δt is over 100 μs in air at 66.7 mbar, a further decrease in electron density apparently leads to decreasing 2nd pulse streamer lengths until at $\Delta t = 1250$ μs they have the same average length as the 1st pulse streamers. It should be pointed out that also during this interval, the 2nd pulse streamers still mostly follow the previous streamer's paths although they may not all match exactly.

After a delay of 1660 μs after the 1st pulse streamers in 66.7 mbar air, the 2nd pulse streamers have the same average length as the first ones. We cannot conclude merely based on the length that now the earlier discharge has no effect on the subsequent event. Stroboscopic images show that some channels in the 2nd pulse streamer discharge sometimes still match the original paths, but when Δt exceeds 10 ms in 66.7 mbar air or 5 ms in 100 mbar air, the two discharges are fully

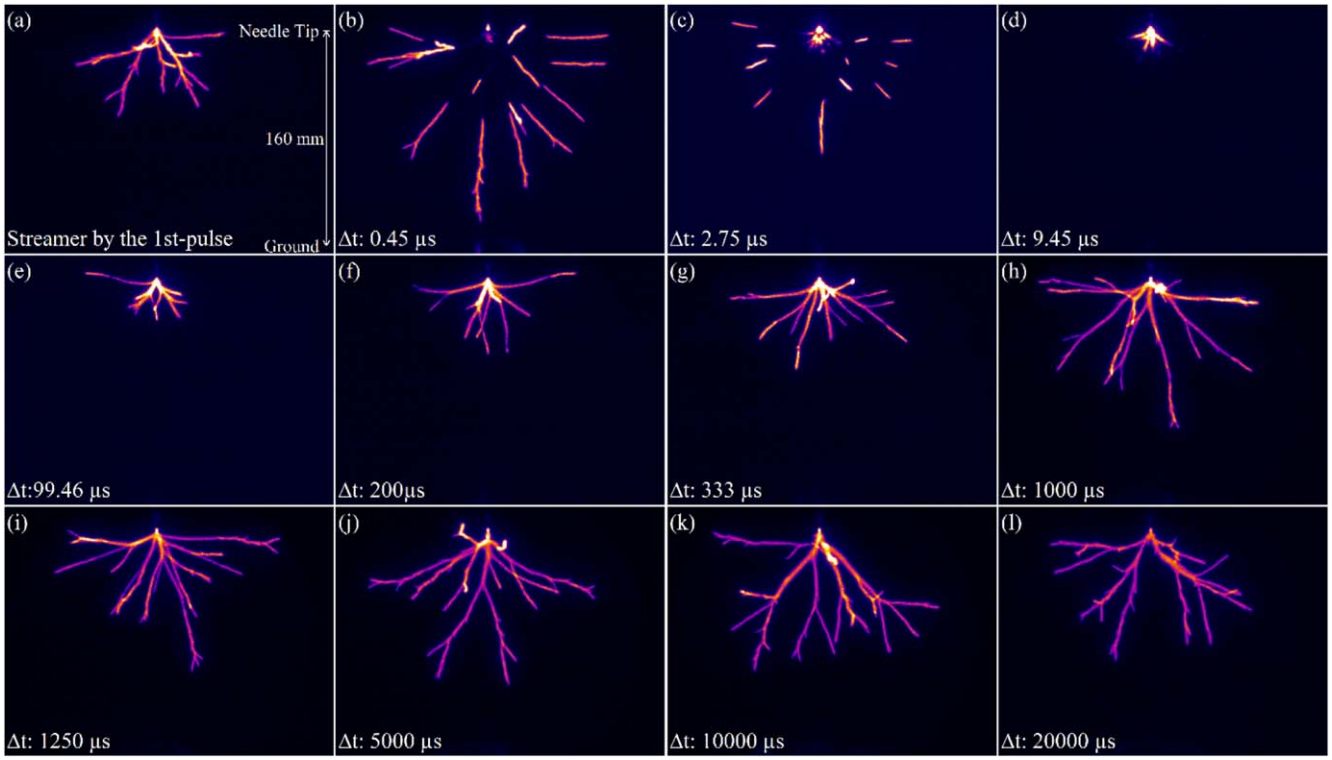

Figure 9. The same plots as in figure 4, but now for 66.7 mbar pure nitrogen with varying pulse-to-pulse delay (Δt) with 6.6 kV voltage amplitude and 500 ns pulse width.

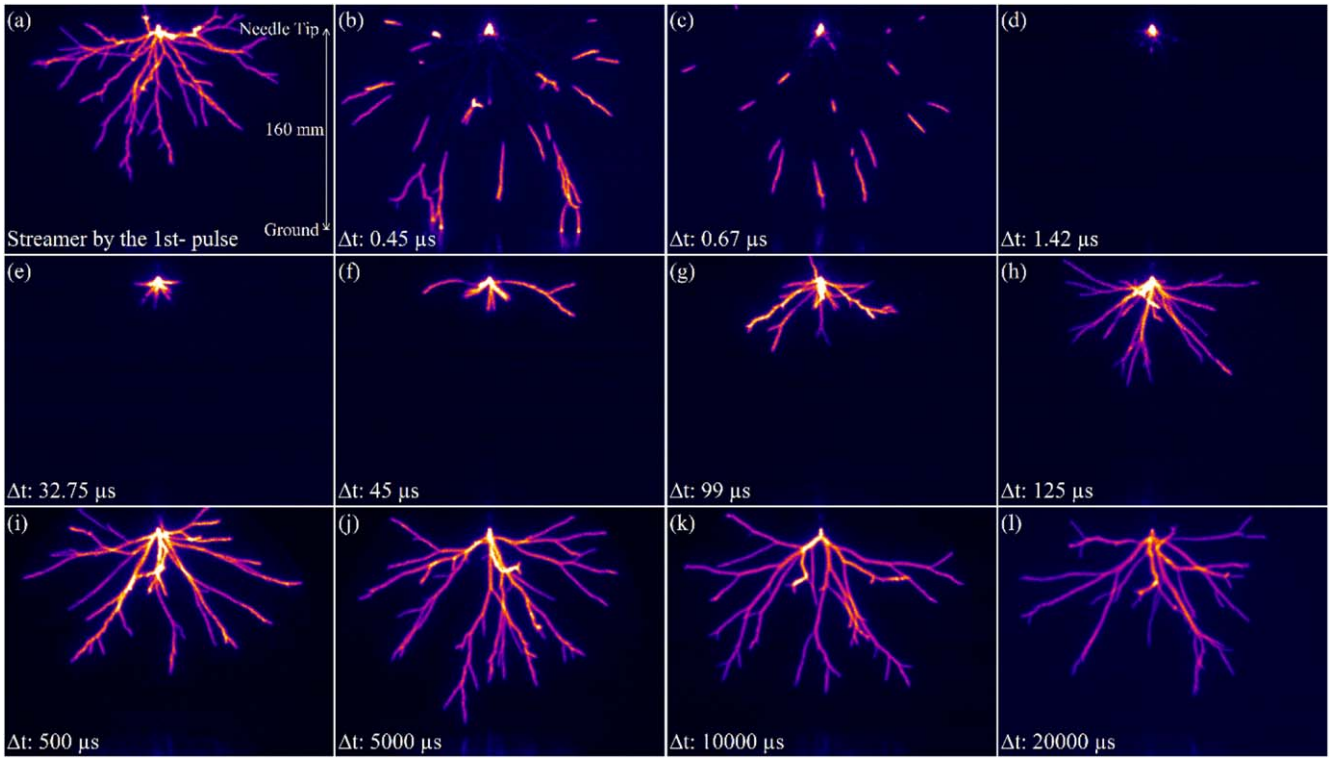

Figure 10. The same as in figure 9, but for 100 mbar pure nitrogen and 8.5 kV voltage amplitude.

independent and no correlation in shape or length can be observed anymore. However, here we still cannot claim that the 2nd pulse streamer or later discharges in repetitive pulse conditions will not be influenced by the previous discharge; the previous discharge definitely supplies a higher background ionization and make the subsequent discharge easier to initiate [4, 6].

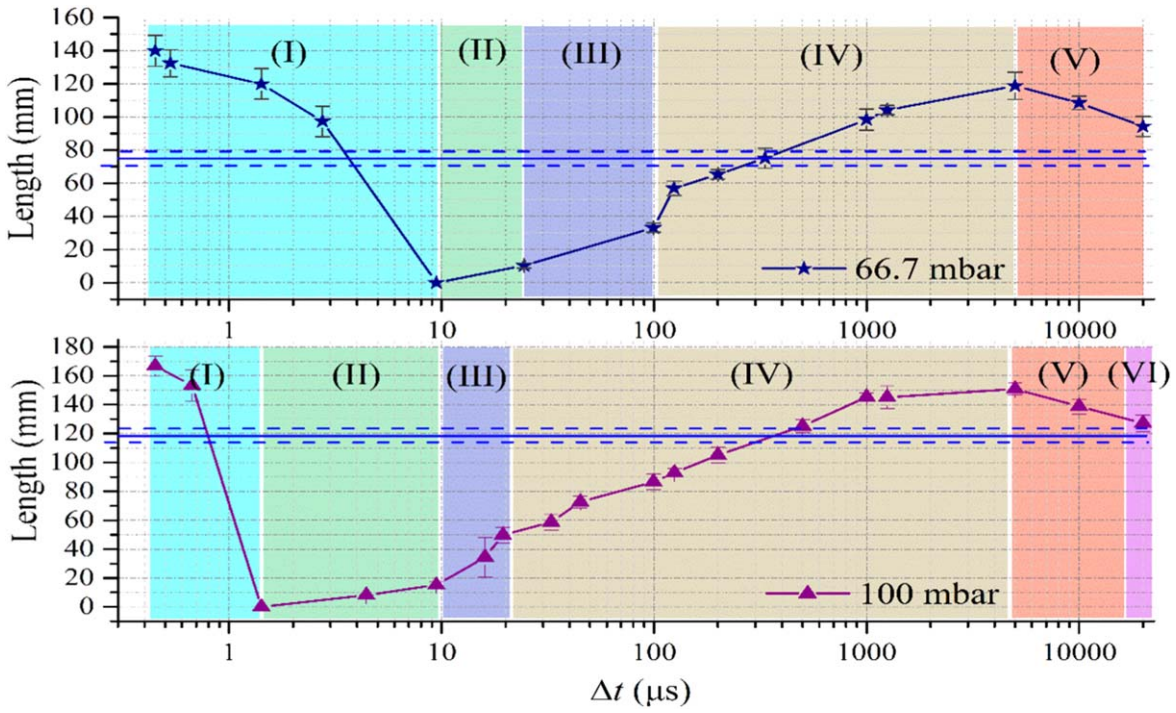

Figure 11. 2nd pulse streamer lengths as a function of Δt in pure nitrogen at 66.7 and 100 mbar. Again, the solid and dashed blue lines represent average and standard deviation of the length of the 1st pulse streamers. Note that for 100 mbar N_2, the total length of the 2nd pulse streamer at stage I is over the electrode gap distance, 160 mm. This is because that straight distance between the needle tip and the end point is greater than the gap distance.

4.2. Nitrogen

The overall progression of positive double-pulse streamer discharges in pure nitrogen for two gas pressures is presented in figures 9 and 10. If we compare them with the discharges in air in figures 4 and 5, it is noticeable that the different stages as a function of pulse delay, Δt, are quite comparable. A general observation in these and other experiments is that all time scales decrease for increasing gas densities due to increased collision rates in denser gases. As a result, for higher pressures, the discharge enters every corresponding stage earlier. The 2nd pulse streamer lengths are shown in figure 11. We now skip the repeated description of the corresponding stages but concentrate on the differences between the two gases.

(a) In nitrogen, 2nd pulse streamers enter every stage with a greater pulse delay time, i.e. greater Δt, than in air at the same pressure. More pronouncedly, the length of the 2nd pulse streamers is still longer than those of the 1st pulse streamers at 66.7 mbar for $\Delta t = 20$ ms, which is the maximum pulse delay in our experiments. Therefore, stage VI is not available for nitrogen at 66.7 mbar in our study. In 100 mbar nitrogen, the 2nd pulse streamer length decreases to almost the length of the 1st pulse streamer for the maximal Δt. The different time scales in nitrogen and air are due to the different electron loss mechanisms. The dominant mechanism in air is electron attachment to oxygen; while in high purity nitrogen only a small (but relevant) oxygen concentration remains. In gas mixtures with high oxygen concentrations (like 20%), electrons quickly attach to oxygen molecules to form negative ions. For the nitrogen we use in the experiment, the impurity is less than 50 ppm, so the attachment rate will be much lower than in air.

(b) Streamers in nitrogen generally have more branches than in air, and they lack a noticeable inception cloud, which is also known from single or repetitive pulsed voltage experiments. The growth of a pronounced inception cloud is due to photoionization in air which smoothness out large electron density gradients in ionization fronts [23, 29]. Experimental and simulation results [4, 30, 31] demonstrate the fact that the streamer branching is less likely to occur if the density of electrons is greater in the streamer ionization front, whether they are produced by photoionization or pre-existing background ionization.

5. Velocities, inception delay and current

5.1. Velocities and inception delay

As presented above in section 4, we find that the 2nd pulse streamers in 66.7 mbar N_2 and artificial air can propagate 66% and 37% longer, respectively, than the 1st pulse streamers. The maximum propagation length is achieved for a pulse delay $\Delta t = 5000$ μs in N_2 and $\Delta t = 100$ μs in air. One could imagine that the 2nd pulse streamers are longer because they are faster—where it should be recalled that the two voltage

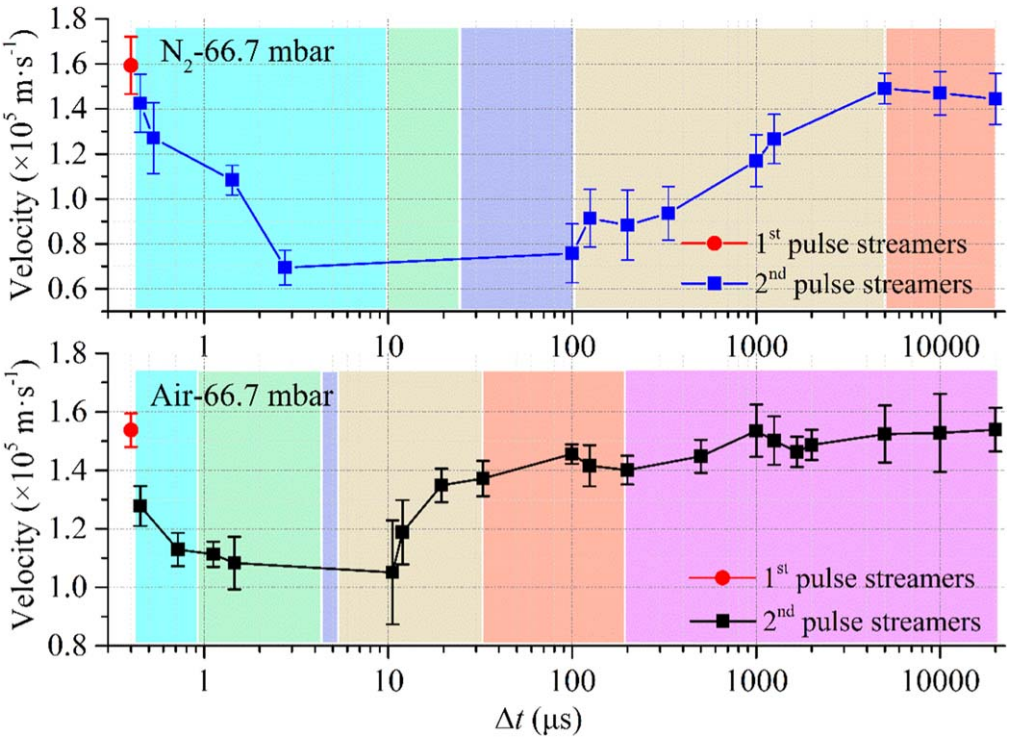

Figure 12. Velocities of the 1st pulse streamers (red dot) and the 2nd pulse streamers (black squares) as a function of Δt in 66.7 mbar N_2 and air. The background colors indicate the same stages as in figures 6 and 11.

pulses are nearly identical, with the second one only slightly lower in amplitude.

We calculate the velocities of the 1st and the 2nd pulse streamers in nitrogen and artificial air both at 66.7 mbar and plot them as a function of the delay Δt as shown in figure 12. The results show that 2nd pulse streamers are not significantly faster than 1st pulse streamers. The velocities of 1st pulse streamers in 66.7 mbar N_2 and air are $(1.59 \pm 0.12) \times 10^5$ m s^{-1} and $(1.53 \pm 0.05) \times 10^5$ m s^{-1} respectively, while the velocities of 2nd pulse streamers are $(1.49 \pm 0.07) \times 10^5$ m s^{-1} for $\Delta t = 5000$ μs in N_2 and $(1.45 \pm 0.04) \times 10^5$ m s^{-1} for $\Delta t = 100$ μs in air. Note that the velocity is not available for 2.75 $\mu s < \Delta t < 100$ μs in nitrogen and 0.72 $\mu s < \Delta t < 5.3$ μs in air, since for these experiments the 2nd pulse streamer length is either too short or the streamers propagate to the side leading to huge statistical errors.

Our result is different from Acker and Penney's findings [12] that subsequent streamer may propagate faster. They found that for repetitive pulses with repetition frequencies as high as 50 kHz, the 16th streamer can be five times faster than the 2nd streamer. Note that in [12] only two photomultipliers (PMT) are used to estimate the average velocity of streamers instead of our more complete velocity profile. Also, in their case, the high repetition frequency may have led to significant gas heating.

Considering the facts that the 2nd pulse streamer in both gases can be longer than the 1st pulse streamers while the 1st pulse streamers are faster, we can here already hypothesize that the 2nd pulse streamers initiate earlier during a pulse than their preceding counterparts. This assumption can be partially supported by the discharge current shown in figure 1 where the conductive current peak appears earlier during the 2nd pulse than during the 1st pulse. We will discuss the capacitive and conductive current in detail in section 5.2.

In order to fully check our hypothesis we use a fixed exposure time (30 ns) and a varying delay time of the camera exposure to determine when the streamers exactly start. We focus on the specific Δt where the 2nd pulse streamer is the longest, namely for $\Delta t = 5000$ μs in N_2 and $\Delta t = 100$ μs in air both at 66.7 mbar. The propagation length as a function of time is indicated in figure 13. Note that here the time denotes the sum of camera delay and gate width of exposure (see schematic demonstration in figure 13) and the propagation length is measured starting from the electrode tip for both gases.

The evolutional morphology of streamers at the inception stage for both gases with varying camera delay times is shown in figure 14. The results show that the 2nd pulse streamer can initiate almost 150 ns earlier than the previous one in 66.7 mbar N_2 (compare figures 14(l) and (n)). Then we find that the 2nd pulse streamer is 33.4 mm longer than the 1st pulse streamer for $\Delta t = 5000$ μs. One should note that the streamer inception has a stochastic nature: figure 13 shows that the length of the 1st pulse streamer in 66.7 mbar N_2 has a huge standard deviation, and that inception occurs much later than for the 2nd pulse streamer. However, in 66.7 mbar air the difference in the inception time is much less pronounced than in N_2. In principle, the 2nd pulse streamer in air can start earlier (with respect to the voltage pulse) than the 1st pulse one, but the length difference is very small especially during the first 120 ns of the pulse. According to figures 14(i)–(l), it is clear that the ionization cloud in 66.7 mbar air experiences

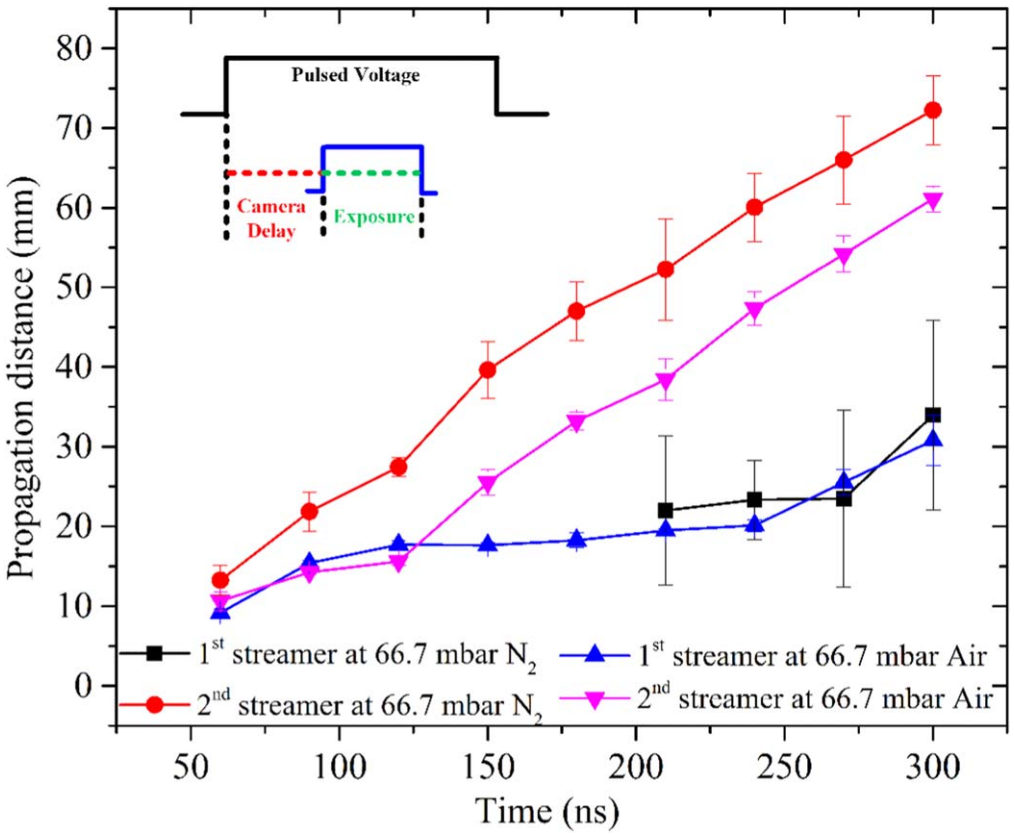

Figure 13. Streamer length as function of time (with respect to the voltage pulse) in 66.7 mbar N_2 and air.

a series of shape changes, from spherical cloud to growing shell, flat shell (with destabilization on the shell edge) before it eventually breaks up into multiple streamer channels. Interestingly, we find that the inception cloud of the 2nd pulse discharge breaks up at least 120 ns earlier than that of the 1st pulse discharge (compare figures 14(l) and (n)), hence the 2nd pulse streamers have more effective propagation time, which results in the observed longer streamer lengths. Together, the reasons that cause the longer length of 2nd pulse streamers are different for air and nitrogen which might indicate different mechanisms in the formation and propagation of 2nd pulse streamers.

At the start of the second pulse, leftover electrons and ions, no matter whether they are produced by previous discharges or by metastable collision, de-excitation, etc, in both gases are much higher compared to the first pulse. This provides seed charges to help the 2nd pulse streamer initiate earlier in N_2, which gives it more time to propagate longer. Meanwhile the electric field in front of the streamer head may be slightly decreased due to shielding by the leftover charged species leading to lower velocities. In air, the leftover electrons and ions increase the destabilization of the inception cloud of the 2nd pulse discharge.

It is necessary to state here that in order to have consistent discharge dimensions we have applied the voltage amplitude shown in table 1. However, we find that the 1st-pulse streamer can bridge the gap in air and nitrogen at 200 and 400 mbar at 17 and 28 kV. For these conditions it is impossible to determine whether the 2nd-pulse streamer is longer than the first. Therefore, the streamer propagation length in section 4 and velocity analysis here do not cover the cases of 200 and 400 mbar.

5.2. Electrical parameters analysis

Figure 15 presents the total current for 1st and 2nd pulse streamers in 100 mbar nitrogen at 8.5 kV as function of time with respect to their voltage pulse. For a pulse delay of $\Delta t = 0.45$ μs, when the 2nd pulse streamer is in the continuation stage (I), the first peak current (the peak in figure 15) of the 2nd pulse streamer is much higher than for the 1st pulse streamer; this indicates that the high conductivity experienced by the 2nd pulse streamer is due to the preceding discharge. However, it is difficult to distinguish the capacitive current from the conductive current according to the shape of the first peak during the 2nd pulse, but the variation in shape of the plateau of the 2nd pulses (the plateau in figure 15) is clear due to conductive current for varying Δt. For larger Δt, the peak of the 2nd pulse decreases to the same height as that of the 1st pulse discharge, while the plateau of the 2nd pulses varies in shape and decreases gradually for 0.45 μs $\leqslant \Delta t \leqslant$ 9.45 μs. This matches the propagation distance analysis of streamers from figure 6, corresponding to stages (iii) to stage (iv). When the 2nd pulse streamer is longer than the 1st pulse streamer, for 125 μs $\leqslant \Delta t \leqslant$ 5000 μs, the plateau increases continuously and its value grows higher than the 1st pulse discharge, which corresponds to a longer propagation distance than the 1st pulse streamer.

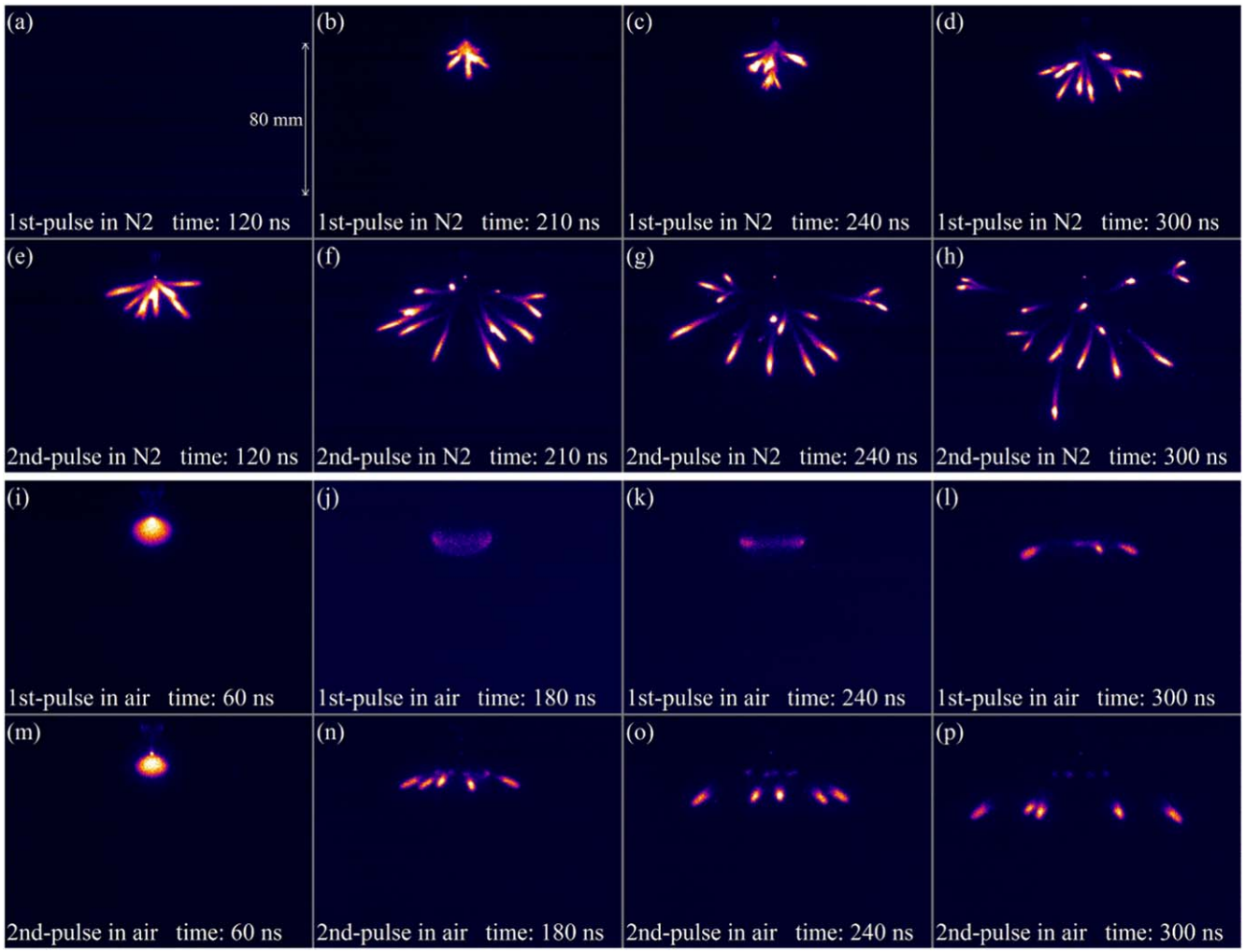

Figure 14. Evolutional morphology of streamers at the inception stage for 66.7 mbar N_2 and air with varying time. The time denotes the sum of camera delay and gate width of exposure (30 ns). (a)–(d): 1st pulse streamer in 66.7 mbar N_2; (e)–(h): 2nd pulse streamer in 66.7 mbar N_2 for $\Delta t = 5000$ μs; (i)–(l): 1st pulse streamer in 66.7 mbar air; (m)–(p): 2nd pulse streamer in 66.7 mbar air for $\Delta t = 100$ μs.

Here we simply calculate the energy during the 1st streamer in 100 mbar air by integration of the discharge power, $\int U(t)\mathrm{i}(t)\mathrm{d}t$. The calculated energy dissipated in the 1st streamer discharge is about 1.4×10^{-4} J. We measured the average diameter of streamer channels in 100 mbar air as 3 mm with 80 mm propagation distance (halfway of the 160 mm electrode gap). Assuming that there are 5 branching channels for each streamer discharge and 30% of the discharge energy is converted to fast heating in 100 mbar air (the density of 1 bar air at room temperature being $1.2\,\mathrm{g\,l^{-1}}$; the specific heat of air being $1.0\,\mathrm{J\,g^{-1}\,K^{-1}}$) [17]. Therefore, we can estimate the temperature in the streamer branches will be elevated by less than 1 K in our experimental conditions. This means that the fast heating processes will not have any significant effect on a subsequent streamer in our case. It is clear that this result is much lower than the calculation from [17], in which the successive streamers finally lead to a spark. In that situation, fast heating is an important contributor to succeeding discharges, but it is very different from our experimental conditions with only two pulses short after each other.

6. Summary, discussion and conclusions

We have investigated how the pulse-to-pulse delay (Δt) influences the subsequent ignition in artificial air and pure nitrogen by double-pulse experiment. We have observed that the 2nd pulse streamer length as a function of Δt can be described with six typical stages.

No 2nd pulse streamers are formed in stage II (2.75 μs $< \Delta t <$ 9.45 μs in 66.7 mbar air and 10 μs $< \Delta t <$ 20 μs in 66.7 mbar N_2) except for some luminescence around the needle tip and the edge of the inception cloud in air. High conductivity around this area likely shields the tip and thereby prevents streamers from initiating and propagating. When this shielding effect starts to diminish, the electric field around the electrode can be enhanced and sideward-propagated streamers can appear (stage III). For larger Δt, the electric field below the tip will gradually increase allowing new streamers to grow. These new streamers follow prior paths of the 1st pulse streamers. This is probably because of the leftover electrons in these paths.

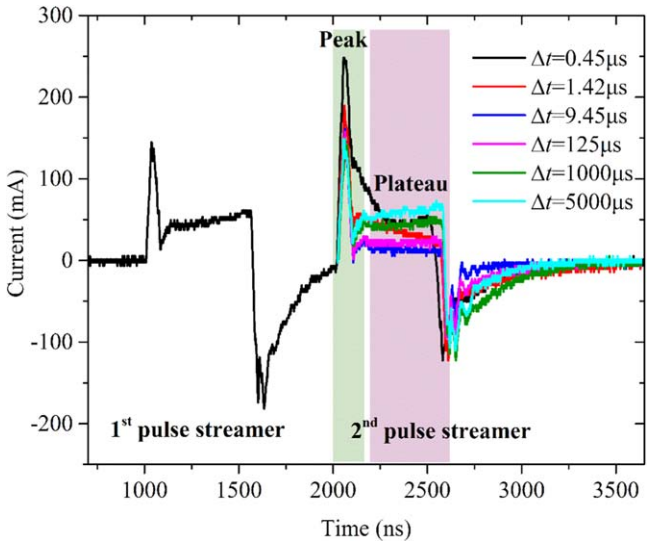

Figure 15. Total current for 1st and 2nd pulse streamers obtained in 100 mbar nitrogen at 8.5 kV. The timing of 2nd pulse streamers is adapted to overlap them in the figure. Two different background colors are used to denote the two parts of total current: the peak consists of capacitive current and conductive current and it is difficult to separate them; but the plateau is believed to indicate the conductive current and is much easier to identify since it should be flat if there is no discharge.

As was discussed in the introduction section, metastable species are a possible physical mechanism that can influence subsequent streamer propagation. However, the exact mechanism for the pulse delay times needs more quantitative analysis and discussion. Our previous simulation results in 2014 [19] based on the local (zero-dimensional) approximation for the plasma chemistry of N_2–O_2 mixtures quantify the roles of electrons, ions and various metastable species. This model incorporates the BOLSIG+ solver and includes 650 reactions of 53 species [32–34], including several superelastic collision reactions. The results show that the electron loss is quick, especially in air due to recombination with positive ions and electron attachment to molecular oxygen (electron attachment can be considered of minor importance in pure nitrogen [24]). The electron density is decreasing monotonously; this means there is no evidence from our simulations that shows that electron density can significantly increase due to collisional reactions or deactivation of metastable states in the plasma decay (the interval between double-pulse). But whether these metastables have further influence on the next discharge, by, for instance, providing easier ionized species, is still an open question and needs more quantitative investigations.

The 2nd pulse streamers are generally longer than their predecessors, by around 66% in 66.7 mbar N_2 and 37% in air at the same pressure. However, we find that this is not caused by a higher propagation velocity nor by fast gas heating of previous channels under our experimental conditions, but by faster initiation of the 2nd pulse streamers. More specifically, we find that the 2nd pulse streamer can initiate almost 150 ns earlier than the previous one (with respect to the voltage pulse) in 66.7 mbar N_2. In 66.7 mbar air, the 2nd pulse streamers start at almost the same time to form the inception cloud but the inception cloud of the 2nd pulse streamer breaks up at least 120 ns earlier than the 1st pulse streamer, hence the 2nd pulse streamers have more effective propagation time and travel longer.

Acknowledgments

This work was supported by National Natural Science Foundation of China (51607139), the Fundamental Research Funds for the Central Universities (Xjj2016012), State Key Laboratory of Electrical Insulation and Power Equipment (EIPE17316), State Key Laboratory of Intense Pulsed Radiation Simulation and Effect (SKLIPR1611) and China Postdoctoral Science Foundation funded project (2016M600793).

ORCID iDs

Y Li https://orcid.org/0000-0001-5424-1764
S Nijdam https://orcid.org/0000-0002-1310-6942

References

[1] Pancheshnyi S V, Starikovskaia S M and Starikovskii A Y 2001 Role of photoionization processes in propagation of cathode-directed streamer *J. Phys. D: Appl. Phys.* **34** 105
[2] Stephens J, Fierro A, Beeson S, Laity G, Trienekens D, Joshi R P, Dickens J and Neuber A 2016 Photoionization capable, extreme and vacuum ultraviolet emission in developing low temperature plasmas in air *Plasma Sources Sci. Technol.* **25** 025024
[3] Pai D Z, Stancu G D, Lacoste D A and Laux C O 2009 Nanosecond repetitively pulsed discharges in air at atmospheric pressure—the glow regime *Plasma Sources Sci. Technol.* **18** 045030
[4] Nijdam S, Wormeester G, van Veldhuizen E M and Ebert U 2011 Probing background ionization: positive streamers with varying pulse repetition rate and with a radioactive admixture *J. Phys. D: Appl. Phys.* **44** 455201
[5] Gago C G, Bordel N, Pereiro R and Sanz-Medel A 2011 Investigation of the afterglow time regime in pulsed radiofrequency glow discharge time-of-flight mass spectrometry *J. Mass Spectrom.* **46** 757–63
[6] Shao T, Sun G, Yan P, Wang J, Yuan W, Sun Y and Zhang S 2006 An experimental investigation of repetitive nanosecond-pulse breakdown in air *J. Phys. D: Appl. Phys.* **39** 2192
[7] Mintusov E, Serdyuchenko A, Choi I, Lempert W R and Adamovich I V 2009 Mechanism of plasma assisted oxidation and ignition of ethylene–air flows by a repetitively pulsed nanosecond discharge *Proc. Combust. Inst.* **32** 3181–8
[8] Lu X and Ostrikov K 2018 Guided ionization waves: the physics of repeatability *Appl. Phys. Rev.* **5** 031102
[9] Raizer Y P 1991 *Gas Discharge Physics* (Berlin: Springer)
[10] Šimek M 2014 Optical diagnostics of streamer discharges in atmospheric gases *J. Phys. D: Appl. Phys.* **47** 463001
[11] Shkurenkov I, Burnette D, Lempert W R and Adamovich I V 2014 Kinetics of excited states and radicals in a nanosecond

pulse discharge and afterglow in nitrogen and air *Plasma Sources Sci. Technol.* **23** 065003
[12] Acker F E and Penney G W 1968 Influence of previous positive streamers on streamer propagation and breakdown in a positive point-to-plane gap *J. Appl. Phys.* **39** 2363–9
[13] Hartmann G and Gallimberti I 1975 The influence of metastable molecules on the streamer progression *J. Phys. D: Appl. Phys.* **8** 670
[14] Lowke J J 1992 Theory of electrical breakdown in air-the role of metastable oxygen molecules *J. Phys. D: Appl. Phys.* **25** 202
[15] Gherardi N and Massines F 2001 Mechanisms controlling the transition from glow silent discharge to streamer discharge in nitrogen *IEEE Trans. Plasma Sci.* **29** 536–44
[16] Pejovic M M and Dimitrijevic B 1982 Electrical breakdown induced by long lived metastable states in nitrogen *J. Phys. D: Appl. Phys.* **15** L87
[17] Geary J M and Penney G W 1974 Temperature as a mechanism for the buildup of successive streamers in low-voltage breakdown *J. Appl. Phys.* **45** 126–34
[18] Popov N A 2011 Fast gas heating in a nitrogen–oxygen discharge plasma: I. Kinetic mechanism *J. Phys. D: Appl. Phys.* **44** 285201
[19] Nijdam S, Takahashi E, Markosyan A H and Ebert U 2014 Investigation of positive streamers by double-pulse experiments, effects of repetition rate and gas mixture *Plasma Sources Sci. Technol.* **23** 025008
[20] Trienekens D J M, Nijdam S and Ebert U 2014 Stroboscopic Images of Streamers Through Air and Over Dielectric Surfaces *IEEE Trans. Plasma Sci.* **42** 2400–1
[21] Nijdam S, Moerman J S, Briels T M P, van Veldhuizen E M and Ebert U 2008 Stereo-photography of streamers in air *Appl. Phys. Lett.* **92** 101502
[22] Briels T M P, van Veldhuizen E M and Ebert U 2008 Positive streamers in air and nitrogen of varying density: experiments on similarity laws *J. Phys. D: Appl. Phys.* **41** 234008
[23] Chen S, Heijmans L C J, Zeng R, Nijdam S and Ebert U 2015 Nanosecond repetitively pulsed discharges in N_2 –O_2 mixtures: inception cloud and streamer emergence *J. Phys. D: Appl. Phys.* **48** 175201
[24] Pancheshnyi S 2015 Photoionization produced by low-current discharges in O_2, air, N_2 and CO_2 *Plasma Sources Sci. Technol.* **24** 015023
[25] Sigmond R S 1984 The residual streamer channel: return strokes and secondary streamers *J. Appl. Phys.* **56** 1355–70
[26] Ono R and Oda T 2003 Formation and structure of primary and secondary streamers in positive pulsed corona discharge-effect of oxygen concentration and applied voltage *J. Phys. D: Appl. Phys.* **36** 1952–8
[27] Briels T M P, Kos J, van Veldhuizen E M and Ebert U 2006 Circuit dependence of the diameter of pulsed positive streamers in air *J. Phys. D: Appl. Phys.* **39** 5201
[28] Nijdam S, Takahashi E, Teunissen J and Ebert U 2014 Streamer discharges can move perpendicularly to the electric field *New J. Phys.* **16** 103038
[29] Teunissen J and Ebert U 2016 3D PIC-MCC simulations of discharge inception around a sharp anode in nitrogen/ oxygen mixtures *Plasma Sources Sci. Technol.* **25** 044005
[30] Takahashi E, Kato S, Sasaki A, Kishimoto Y and Furutani H 2011 Controlling branching in streamer discharge by laser background ionization *J. Phys. D: Appl. Phys.* **44** 75204
[31] Luque A and Ebert U 2011 Electron density fluctuations accelerate the branching of positive streamer discharges in air *Phys. Rev.* E **84** 046411
[32] Pancheshnyi S, Eismann B, Hagelaar G J M and Pitchford L C 2008 *ZDPlasKin Zero-Dimensional Plasma Kinetics solver* (Toulouse, France: LAPLACE, CNRS-UPS-INP,University of Toulouse)
[33] Flitti A and Pancheshnyi S 2009 Gas heating in fast pulsed discharges in N_2–O_2 mixtures *Eur. Phys. J.—Appl. Phys.* **45** 285201
[34] Capitelli M, Ferreira C M, Gordiets B F and Osipov A I 2013 *Plasma Kinetics in Atmospheric Gases* (Berlin, Heidelberg: Springer Science & Business Media)